Available online at www.sciencedirect.com

ScienceDirect

Current Opinion in Electrochemistry

Review Article

A formalism to compare electrocatalysts for the oxygen reduction reaction by cyclic voltammetry with the thin-film rotating ring-disk electrode measurements

Vito Di Noto[1,2], Gioele Pagot[1,3], Enrico Negro[1,3], Keti Vezzù[1,2], Pawel J. Kulesza[4], Iwona A. Rutkowska[4] and Giuseppe Pace[5]

Abstract

This report describes a general method to correlate the features determining the performance of an electrocatalyst (EC), including the accessibility of O_2 to the active sites and the kinetic activation barrier, with the outcome of conventional electrochemical experiments. The method has been implemented for oxygen reduction reaction ECs by cyclic voltammetry with the thin-film rotating ring-disk electrode (CV-TF-RRDE) setup. The method: (i) does not rely on the simplifications associated with the Butler-Volmer kinetic description of electrochemical processes and (ii) does not make assumptions on the specific features of the EC, allowing to compare accurately the kinetic performance of oxygen reduction reaction ECs with completely different chemistry. Finally, with respect to other widespread figures of merit (*e.g.*, the half-wave potential $E_{1/2}$), the figure of merit here proposed, $E(j_{Pt}(5\%))$, allows for much more accurate comparisons of the kinetic performance of ECs.

Addresses

[1] Section of Chemistry for the Technology (ChemTech), Department of Industrial Engineering, University of Padova, Via Marzolo 9, I-35131, Padova, PD, Italy

[2] Consorzio Interuniversitario Nazionale per la Scienza e Tecnologia dei Materiali - INSTM, Via Marzolo 1, I-35131, Padova, PD, Italy

[3] Centro Studi di Economia e Tecnica dell'Energia Giorgio Levi Cases, Via Marzolo 9, I-35131, Padova, PD, Italy

[4] Faculty of Chemistry, University of Warsaw, Pasteura 1, PL-02-093, Warsaw, Poland

[5] Consiglio Nazionale delle Ricerche, Istituto di Chimica della Materia Condensata e di Tecnologie per l'Energia, Italy

Corresponding authors: Di Noto, Vito (vito.dinoto@unipd.it); Pagot, Gioele (gioele.pagot@unipd.it)

Current Opinion in Electrochemistry 2022, **31**:100839

This review comes from a themed issue on **Energy Transformation**

Edited by **Bruno G. Pollet** and **Jacob Joseph Lamb**

For a complete overview see the Issue and the Editorial

Available online 14 September 2021

https://doi.org/10.1016/j.coelec.2021.100839

Keywords

Comparison of kinetic performance, Oxygen reduction reaction, Thin-film rotating ring-disk electrode, Accessibility, Activation barrier.

Introduction

The oxygen reduction reaction (ORR) is exploited in the operation of several electrochemical energy conversion and storage devices, such as metal-air batteries (*e.g.*, Li-air, Zn-air, Al-air, and so on.) [1–5] and fuel cells (*e.g.*, proton exchange membrane fuel cells, anion-exchange membrane fuel cells, and so on) [6–11]. In these systems, the ORR is very often the slowest electrochemical process, yielding large overpotentials and thus degrading the overall energy efficiency of the final device. In this concern, the development of suitable electrocatalysts (ECs) able to promote the ORR is of fundamental importance. Such ECs are able to abate the activation energy (E_a) of the process, typically by introducing intermediate step reactions characterized by a lower E_a [12,13]. The best performing ORR ECs are based on Pt or other platinum group metals (PGMs), which unfortunately are not abundant in Earth's crust and thus are classified as critical raw materials. This supply bottleneck [14,15] is a crucial issue, especially in the perspective of using PGM-based ECs in the fabrication of high-energy and high-power electrochemical energy conversion devices on a large scale (*e.g.*, for automotive applications). A detailed study able to shed light on the operating mechanism of an EC requires the use of a large number of complex techniques, and when studied '*in situ*,' the assembly and the test of a complete device. Therefore, the development of simple methods able to provide information on the crucial properties of the ECs is highly welcome. Cyclic voltammetry with the thin-film rotating ring-disk electrode (CV-TF-RRDE) is one of the most powerful methods for the investigation of electrochemical systems, especially in the case of heterogeneous reactions [16]. Indeed, the CV-TF-RRDE technique allows to study the kinetics of an electrochemical process promoted by an EC (that is typically deposited onto the tip of the working

electrode) limiting as much as possible the formation of interfaces at the EC/electrolyte [16] and the influence of complex phenomena, such as the charge and mass transport events on measured parameters. Indeed, in CV-TF-RRDE measurements charge and mass transport phenomena are not time-dependent; thus, their analysis is quite simple. The ORR mechanism is significantly influenced by a number of conditions such as: (i) the reaction environment (*e.g.*, aqueous or organic) and (ii) the pH (*e.g.*, acidic, neutral, or alkaline) [17,18]. The local environment is able to modulate both: (i) the kinetic parameters of the reaction mechanism; and (ii) the products of the ORR, thus affecting the reaction pathway. Indeed, depending on the number of electrons exchanged during the ORR: (a) in aqueous conditions, water (H_2O) or hydrogen peroxide (H_2O_2) can be formed [19,20]; while (b) in nonaqueous media, metal oxide, peroxide, superoxide, or hydroxide species (*e.g.*, Li_2O, Li_2O_2, LiO_2, LiOH) are obtained [21–23]. Moreover, in the literature there is not a unanimous consensus on how to determine the parameters to gauge the activity of ECs in the ORR. In particular, it is yet to be agreed on the current density at which the ORR onset potential (E_{onset}) is to be determined. The half-wave potential ($E_{1/2}$) is often used as a figure of merit to assess the overall performance of ECs in the ORR [24,25]. However, it is highlighted that $E_{1/2}$ values are generally determined in the mixed kinetic-diffusion region, thus leading to a lower accuracy in the estimation of the ORR kinetic parameters of the ECs [26].

In this report, a simple and general method is proposed to determine and compare suitable parameters describing the efficiency in the kinetic regime of a broad number of chemically different ECs for the ORR. This method is based on CV-TF-RRDE measurements and allows us to study and compare ECs operating in both aqueous and nonaqueous media. The method is: (a) easily transferable to a large variety of electrochemical reactions which are exploited in several energy conversion and storage systems; and (b) based on a general physicochemical formalism which allows to detect and interpret the experimental parameters which are diagnostic for a rigorous comparison of kinetic performance of different ECs. The proposed general physicochemical framework accounts for the kinetic conversion of mass flow throughout the electrode into electrons. This target is achieved by describing the redox process occurring at the electrode in terms of a general kinetic rate concept. Here no Butler-Volmer (BV) description of the process occurring at the electrode is assumed. Indeed, as clearly reported elsewhere [27], the BV equation is the result of the $k_{red} = k_{ox} = k^0$ approximation, where k_{red} and k_{ox} are the elementary reduction and oxidation rate constants, respectively, and k^0 is the 'standard rate constant' characterizing the exchange current (i_0). The motivation is that in real ECs: (a) in general, it is observed that $k_{red} \neq k_{ox} \neq k^0$; and (b) to compare kinetically different materials exhibiting a very different chemistry is crucial to determine both k_{red} and k_{ox}. Central to this approach is the idea that in a redox process an EC is conceptually a material able to reduce the energy barrier going from the reactants to the activated complex $\Delta G^{\ddagger}_{0,ox}$ and in the opposite process from the products into the activated complex $\Delta G^{\ddagger}_{0,red}$ (see Scheme 1).

Another approximation which in the derivation of the BV equation resulted in the $k_{red} \neq k_{ox} \neq k^0$ condition and which is difficult to obtain in real ECs is the assumption that the bulk concentration of the oxidized reagent species (*e.g.*, O_2) is equivalent to that of the reduced products (*e.g.*, H_2O) so that the forward and backward rate constants in the ORR are coincident [27].

Owing to these motivations, herein a physicochemical formalism is proposed which, tightly to the experimental conditions usually used in the CV-TF-RRDE measurements, rationalizes: (a) the measuring strategy adopted for the correct determination of the kinetic catalytic ability of the ECs; and (b) the method used to carry out a rigorous comparison between catalytic abilities of ECs based on completely different chemistries.

Description of the formalism

The following general redox process converts an oxidized specie (Ox) into a reduced specie (Red) on exchange of n_{tot} electrons (see Eq. (1)):

$$Ox + n_{tot}e^- \rightarrow Red \tag{1}$$

In the presence of a net reduction current, the overall rate, ν_{net}, of the process is given by

$$\nu_{net} = k_{red}C_{ox}(0,t) - k_{ox}C_{red}(0,t) \tag{2}$$

where k_{red} and k_{ox} are the rate constants of reduction and oxidation processes, respectively. $C_{ox}(0,t)$ and $C_{red}(0,t)$ are the concentration of the oxidized and reduced species on the ECs' surface (x = 0) at time t. Each rate constant k_i (i = red, ox) can be expressed by Arrhenius equations:

$$k_i = f_i exp\left(-\frac{\Delta G_i^{\ddagger}}{RT}\right) \tag{3}$$

where R is the ideal gas constant, T the absolute temperature, f_i the decay rate to the products, and $\Delta G_i^{\ddagger}$ the activation barrier of either the forward (reduction, i = red) or the backward (oxidation, i = ox) processes. As elsewhere described [27], when the electrode is at a potential E, the activation barriers $\Delta G_i^{\ddagger}$ (i = red, ox) are

Scheme 1

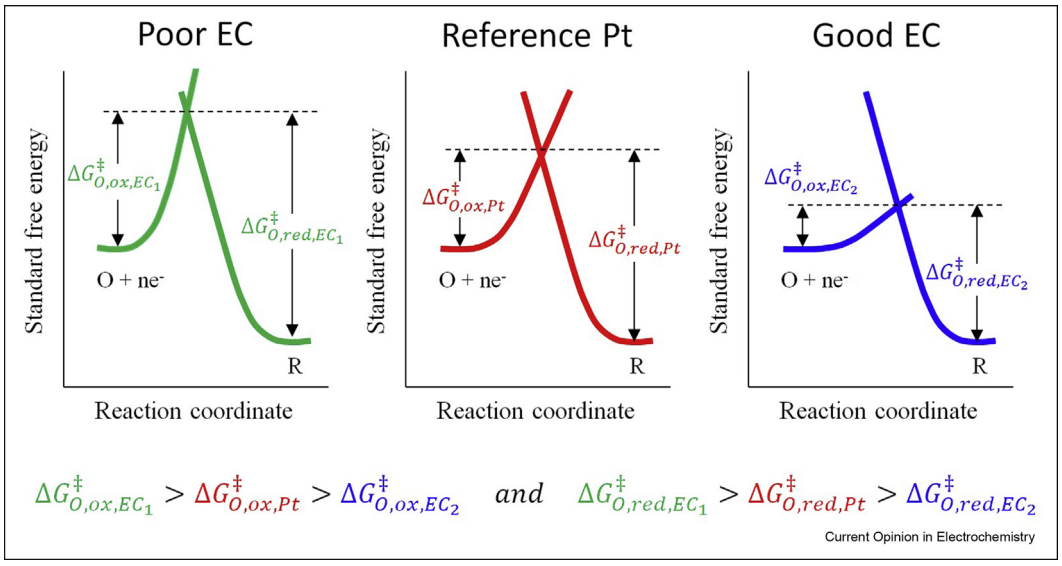

Energy barriers of the EC in the O + ne⁻ → R reduction reaction.

$$\begin{cases} \Delta G^{\ddagger}_{red} = \Delta G^{\ddagger}_{0,red} + \dfrac{\alpha nF}{RT}\left(E - E^{0'}\right) \\ \Delta G^{\ddagger}_{ox} = \Delta G^{\ddagger}_{0,ox} - \dfrac{(1-\alpha)nF}{RT}\left(E - E^{0'}\right) \end{cases} \quad (4)$$

where F the Faraday constant, $E^{0'}$ the formal electrode potential, $\Delta G^{\ddagger}_{0,i}$ (i = red, ox) the activation barrier at the formal electrode potential $E^{0'}$, α the symmetry factor, and n the number of exchanged electrons in the rate-determining step of the redox process. By substituting Eq. (4) into Eq. (3), k_{red} and k_{ox} become

$$\begin{cases} k_{red} = f_{red} exp\left(-\dfrac{\Delta G^{\ddagger}_{0,red}}{RT}\right) exp\left[-\dfrac{\alpha nF}{RT}\left(E - E^{0'}\right)\right] \\ k_{ox} = f_{ox} exp\left(-\dfrac{\Delta G^{\ddagger}_{0,ox}}{RT}\right) exp\left[\dfrac{(1-\alpha)nF}{RT}\left(E - E^{0'}\right)\right] \end{cases} \quad (5)$$

where the first two terms in each of these equations yield a product that is independent of electrode potential and which depends only on the structure, morphology, and composition of the ECs.

The substitution of Eq. (5) into Eq. (2) also considering

$$j_{red} = \frac{n_{tot}F}{A} v_{net} \quad (6)$$

where A is the area of the electrode yields

$$j_{red} = \frac{n_{tot}F}{A}\left[f_{red} exp\left(-\frac{\Delta G^{\ddagger}_{0,red}}{RT}\right) exp\left[-\frac{\alpha nF}{RT}\left(E - E^{0'}\right)\right] C_{ox}(0,t) - f_{ox} exp\left(-\frac{\Delta G^{\ddagger}_{0,ox}}{RT}\right) exp\left[\frac{(1-\alpha)nF}{RT}\left(E - E^{0'}\right)\right] C_{red}(0,t)\right] \quad (7)$$

Now, if we consider that the ORR is very sluggish, and the current density of the reverse oxidation process during ORR is negligible owing to the large overpotentials, Eq. (7) becomes

$$j_{red} = \frac{n_{tot}F}{A}\left[C_{ox}(0,t) f_{red} exp\left(-\frac{\Delta G^{\ddagger}_{0,red}}{RT}\right) exp\left[\frac{\alpha nF\eta}{RT}\right]\right] \quad (8)$$

where $\eta = E^{0'} - E$ is the overpotential with respect to the formal electrode potential $E^{0'}$. For the sake of comparison, Eq. (8) can be generalized, and by simple algebraic manipulations, the overpotential η_i both for a benchmark EC (i = Pt) and for the EC under study (i = EC) can be expressed as

$$\eta_i = T_{sl,i} ln\left(\frac{j_i(\eta_i)A}{n_{tot,i}\, FC_{ox,Pt}(0,t)\, f_{red,i}}\right) + T_{sl,i}\left(\frac{\Delta G^{\ddagger}_{0,red,i}}{RT}\right) \tag{9}$$

$T_{sl,i} = \frac{RT}{\alpha_i n_i F}$ coincides exactly with the η_i *vs.* $\log(j_i)$ Tafel slope. By using Eq. (9) and considering the 'benchmark' a commercial state-of-the-art platinum EC, the difference in the ORR overpotentials is evaluated as follows:

$$\begin{aligned}\eta_{EC} - \eta_{Pt} = &\left[T_{sl,EC} ln\left(\frac{j_{EC}(\eta_{EC})A}{n_{tot,EC} FC_{ox,EC}(0,t) f_{red,EC}}\right)\right. \\ &\left. + T_{sl,EC}\left(\frac{\Delta G^{\ddagger}_{0,red,EC}}{RT}\right)\right] \\ &- \left[T_{sl,Pt} ln\left(\frac{j_{Pt}(\eta_{Pt})A}{n_{tot,Pt} FC_{ox,Pt}(0,t) f_{red,Pt}}\right)\right. \\ &\left. + T_{sl,Pt}\left(\frac{\Delta G^{\ddagger}_{0,red,Pt}}{RT}\right)\right]\end{aligned} \tag{10}$$

Eq. (10) is a powerful tool which permits the development of a simple and straightforward method to compare in the kinetic region the ORR performance of different types of ECs with respect to that of a Pt benchmark. To achieve this target, it is first necessary to select the best condition to measure the ORR kinetic parameters of the Pt benchmark. This is obtained by determining in the 'CV-TF-RRDE' ORR curve a current density, $j_{Pt}(5\%) = \frac{5}{100} j_{Pt,d}$, corresponding to 5% of the diffusion-limited current density ($j_{Pt,d}$) at E ≈ 0.35 V *vs.* RHE, the reversible hydrogen electrode (see Figure 1). It must be pointed out that the acquisition of a CV-TF-RRDE measurement is very delicate and that it is fundamental to properly determine the kinetic parameters of the ORR for an EC. Indeed, it is well known that the ORR kinetics on Pt strongly depends on several factors (*e.g.*, potential scan direction, electrode pretreatment, electrolyte composition, and so on.) [28–31]. Thus, a standard 'benchmark' condition must be selected. In this way, CV-TF-RRDE results can be reproduced independently from the specific operator who is carrying out the measurements.

The motivation is clear if we consider that:

i. the performance of an ORR EC can be evaluated by fixing in the ORR the yield in current of a specific amount of consumed O_2;
ii. it is crucial to monitor the electrocatalytic kinetic parameters such as the activation energy barrier and the symmetry factor characterizing this process;
iii. in a reference EC, the most suitable condition in the kinetic regime to convert an amount of O_2 into current is to monitor the electrode potential at $j_{Pt}(5\%)$.

On these bases, a given EC can be studied in the ORR with respect to the Pt benchmark by evaluating the difference in the overpotentials when they yield the same current density, that is, $j_{Pt}(5\%)$:

$$j_{EC}(\eta_{EC}) = j_{Pt}(\eta_{Pt}) = j_{Pt}(5\%) \tag{11}$$

Considering that

$$T_{sl,i} = \frac{RT}{\alpha_i n_i F} = \frac{RT}{F}\omega_i \text{ with } \omega_i = \frac{1}{\alpha_i n_i} = \frac{1}{\gamma_i} \tag{12}$$

ω_i is the 'selectivity parameter' (i = EC, Pt) and $\gamma_i = \alpha_i n_i$ the transfer coefficient [32]. Since in the ORR $0 \leq n_i \leq 4$ and $0 \leq \alpha_i \leq 1$, then it results that $0 \leq \gamma_i \leq 4$ and $0.25 \leq \omega_i \leq \infty$. By substituting Eq. (11) and Eq. (12) into Eq. (10), it is possible to correlate the overpotential of the EC to that of Pt reference as follows:

Figure 1

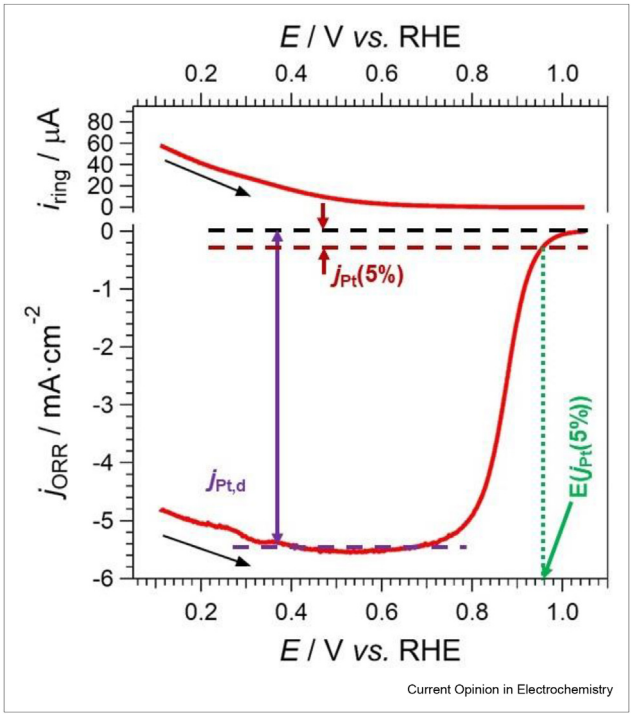

The concept of the E(j_{Pt}(5%)) value.

$$\eta_{EC} = \eta_{Pt} + \frac{RT}{F}\left\{(\omega_{EC} - \omega_{Pt})[ln(j_{Pt}(5\%)) + ln(A) - lnF] + \left[ln\frac{(A_{EC})^{\omega_{EC}}}{(A_{Pt})^{\omega_{Pt}}}\right] - \left[ln\frac{\left(n_{tot,EC}f_{red,EC}\right)^{\omega_{EC}}}{\left(n_{tot,Pt}f_{red,Pt}\right)^{\omega_{Pt}}}\right] - \left[ln\frac{\left(C_{ox,EC}(0,t)\right)^{\omega_{EC}}}{\left(C_{ox,Pt}(0,t)\right)^{\omega_{Pt}}}\right] + \left[\frac{\omega_{EC}\Delta G^{\ddagger}_{0,red,EC} - \omega_{Pt}\Delta G^{\ddagger}_{0,red,Pt}}{RT}\right]\right\} \quad (13)$$

Eq. (13) can be rewritten in the following simple form:

$$\eta_{EC} = \eta_{Pt} + \eta_{exp} + \eta_s + \eta_A + \eta_{kin} \quad (14)$$

where

- η_{Pt} is the ORR overpotential of the Pt benchmark at $j_{Pt}(5\%)$.
- $\eta_{exp} = \frac{RT}{F}\{(\omega_{EC} - \omega_{Pt})[ln(j_{Pt}(5\%)) + ln(A) - lnF]\}$ is the overpotential which accounts for the experimental conditions (*e.g.*, temperature, area of the electrode).
- $\eta_s = -\frac{RT}{F}\left\{ln\frac{(n_{tot,EC}f_{red,EC})^{\omega_{EC}}}{(n_{tot,Pt}f_{red,Pt})^{\omega_{Pt}}}\right\}$ is the 'selectivity overpotential.' This depends on the total number of electrons involved in the process and on the reaction decay rate to the products. When the total number of electrons exchanged and the decay rate to the products of a given EC are smaller than the corresponding figures exhibited by the Pt benchmark, η_{EC} increases.
- $\eta_A = -\frac{RT}{F}\left[ln\frac{(C_{ox,EC}(0,t))^{\omega_{EC}}}{(C_{ox,Pt}(0,t))^{\omega_{Pt}}}\right]$ is the 'accessibility overpotential'. This term accounts for the actual concentration of O_2 adsorbed on the surface of the active sites of a given EC with respect to that of the Pt benchmark. When the active sites of the EC are 'more accessible' than those of the Pt benchmark, η_A decreases. As shown in the following, η_A might be relevant also at very low current densities (*e.g.*, at $j_{Pt}(5\%)$), that is, in conditions when usually the issues arising from the mass transport of reactants and products are considered negligible.
- $\eta_{kin} = \left[\frac{\omega_{EC}\Delta G^{\ddagger}_{0,red,EC} - \omega_{Pt}\Delta G^{\ddagger}_{0,red,Pt}}{F}\right]$ is related to the difference in energy activation barriers between the EC and the Pt benchmark. If the energy barrier of the EC is larger than that of the Pt benchmark, η_{EC} increases.

Eq. (14) can be used to study the ORR process in a variety of environmental conditions (*e.g.*, in an acidic medium, in an alkaline medium, in an organic solvent) and involving a number of different products (*e.g.*, water, peroxide, superoxide, and so on). Finally, the selectivity parameter ω_i, that is, the parameter that describes the electrochemical behavior of the EC and of the Pt benchmark in the process of interest, can be determined experimentally from the Tafel slope of the ORR at a current density close to $j_{Pt}(5\%)$. This allows to reduce the number of undefined parameters in Eq. (13). Taken all together, Eq. (13) and Eq. (14) are crucial results to gauge which features of the EC are the most relevant to reduce the overall overpotential η_{EC} in the ORR.

It is found that in aqueous environments (either acidic or alkaline), a wide variety of ECs (both comprising platinum and 'Pt-free') exhibit in the ORR at room temperature and at very low current densities ($\approx j_{Pt}(5\%)$), a Tafel slope of the same order of magnitude (*ca.* 70 mV dec^{-1}) [16]. As elsewhere reported, for a wide variety of ECs in these conditions the ORR is bottlenecked by the first electron transfer from the electrode to an O_2 molecule adsorbed on the active sites of the EC [16,32,33]. In this case, O_2 adsorption events take place in accordance with the Temkin isotherm [16,32,33].

$$\omega_{Pt} = \omega_{EC} = \omega \cong 1.18 \quad (15)$$

In addition, if we consider that the free-energy surface in the vicinity of the activated state bottlenecking the ORR typically does not change significantly for different ECs [34], we can assume that $f_{red,EC} \approx f_{red,Pt}$. As a result, Eq. (13) can be rewritten as follows:

$$\eta_{EC} = \eta_{Pt} - T_{sl}ln\left(\frac{n_{EC,tot}}{n_{Pt,tot}}\right) - T_{sl}ln\left(\frac{C_{ox,EC}(0,t)}{C_{ox,Pt}(0,t)}\right) + \frac{\omega}{F}\left(\Delta G^{\ddagger}_{0,red,EC} - \Delta G^{\ddagger}_{0,red,Pt}\right) = \eta_{Pt} + \eta_s + \eta_A + \eta_{kin} \quad (16)$$

where, as described previously, we can assume T_{sl} as the Tafel slope of the ORR (*ca.* 70 mV dec^{-1}).

Impact on η_{EC} of the different overpotentials at E(j_{Pt}(5%))

In Eq. (16) η_s, η_A, and η_{kin} play a crucial role in the modulation of the magnitude of η_{EC} at $j_{Pt}(5\%)$. To gauge the relative impact of these overpotentials on η_{EC}, the profiles of η_s, η_A, and η_{kin} are simulated adopting the following general conditions. For the η_s of the Pt benchmark at E($j_{Pt}(5\%)$), it is assumed a total number of 4 electrons ($n_{tot} = 4$). For the other ECs, $n_{tot,EC}$ can typically range between 2 (ORR EC yielding only H_2O_2) and 4 (ORR EC yielding only water). It should be noted that in organic solvents the ORR can also yield the superoxide ion, corresponding to the exchange of only one electron [21]. Hence, in general, the following boundary conditions are adopted:

$$0.5 \leq \left(\frac{n_{EC,tot}}{n_{Pt,tot}}\right) \leq 1 \tag{17}$$

For the evaluation of η_A, it is reasonable to admit that the density of O_2 adsorbed on the surface of the active sites: (i) depends on the composition, structure, and morphology of the EC and (ii) is different from that of the Pt benchmark. On these bases, it is reasonable to assume that

$$0.01 \leq \left(\frac{C_{ox,EC}(0,t)}{C_{ox,Pt}(0,t)}\right) \leq 5 \tag{18}$$

For the evaluation of η_{kin}, studies elsewhere reported estimate for the ORR on a Pt nanoparticle an activation barrier on the order of 1.13 eV (*ca.* 109 kJ mol^{-1}) [35]. Starting from this $\Delta G^{\ddagger}_{0,red,Pt}$ value for the benchmark, in the simulation of η_{kin} it is reasonable to consider that $\Delta G^{\ddagger}_{0,red,EC}$ ranges within the following boundary conditions:

$$\begin{aligned}&\Delta G^{\ddagger}_{0,red,Pt} - 50\% \cdot \Delta G^{\ddagger}_{0,red,Pt} \leq \Delta G^{\ddagger}_{0,red,EC} \leq \Delta G^{\ddagger}_{0,red,Pt} \\ &+50\% \cdot \Delta G^{\ddagger}_{0,red,Pt}.i.e. \\ &54.51\ kJ \cdot mol^{-1} \leq \Delta G^{\ddagger}_{0,red,EC} \leq 163.5\ kJ \cdot mol^{-1}\end{aligned} \tag{19}$$

The results of the simulations are displayed in Figure 2. The value of T_{sl} is set to 70 mV dec^{-1}, corresponding to $\omega = 1.18$ (see Eq. [15]).

Figure 2 demonstrates that η_s has little impact on the overall overpotential of the EC. In detail, it results that the ORR overpotential characterizing an EC able to reduce O_2 exclusively to hydrogen peroxide ($n_{tot} = 2$) would be only *ca.* 48 mV larger than that of an EC able to convert O_2 exclusively to water ($n_{tot} = 4$). At the level of investigation of this work, the possible formation of mixed potentials owing to the establishment of the O_2/H_2O_2 redox couple was not considered. The impact of the accessibility overpotential (η_A) on η_{EC} is much more relevant. Indeed, with respect to the Pt benchmark, a 10-fold decrease of the O_2 density on the electrode surface of the EC would trigger an increase in the overpotential of *ca.* 160 mV. At $j_{EC}(5\%)$, η_{kin} is the most important contribution to η_{EC}. Indeed, if the ORR activation barrier of an EC is only 25 kJ mol^{-1} larger than that of the Pt benchmark, the ORR overpotential increases by more than 300 mV. This is the difference commonly existing experimentally between the best ORR Pt-based ECs and most of the poor 'Pt-free' ECs.

Application of the formalism to real cases

The framework described in Section 3 is implemented by means of conventional ORR measurements in the

Figure 2

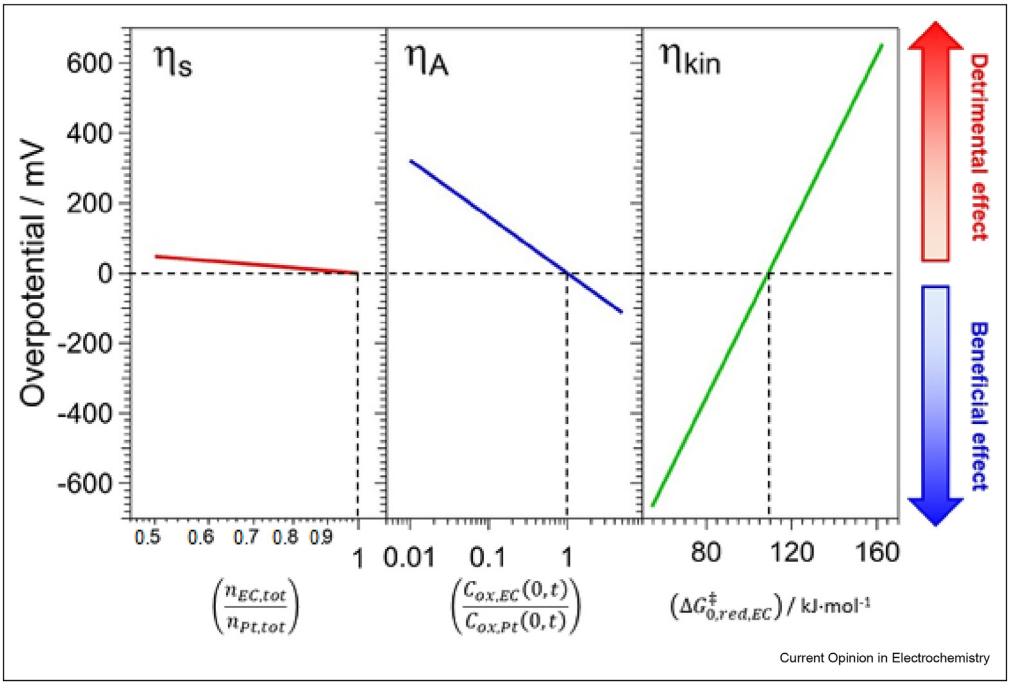

Simulation on boundary conditions expressed by Eq. (17), Eq. (18), and Eq. (19) of η_s (left panel), η_A (center panel), and η_{kin} (right panel) values, respectively.

CV-TF-RRDE setup. A detailed discussion of the CV-TF-RRDE setup, of the approaches that are adopted to bind the EC to be tested on the RRDE tip, and of the rationale underlying the selection of the experimental parameters (*e.g.*, temperature, rotation rate of the RRDE, composition of the support electrolyte), is outside the scope of this work and can be found in the literature [36]. The data analysis starts by determining the ORR faradic currents adopting the procedures described elsewhere [16]. iR correction is carried out, allowing for the accurate determination of the electrode potential accounting for the ohmic drops in the system. In conventional aqueous media, both under acidic and alkaline media, $j_{Pt,d}$ is *ca.* 6 mA cm^{-2} as the RRDE is spun at 1600 rpm [37,38]. Accordingly in these conditions, that are adopted herein, $j_{Pt}(5\%)$ is typically on the order of *ca.* 0.3 mA cm^{-2}. This latter value is: (i) large enough to ensure that the errors introduced on the removal of the capacitive currents are small; and (ii) small enough to justify the neglect of the corrections owing to mass transport arising from the RRDE experimental setup. The possible electrocatalytic effects associated with the ionomer and the EC loading on $j_{EC}(5\%)$ can be revealed by measuring this latter parameter as a function of the ionomer and the EC loading in the electrocatalytic layer covering the RRDE tip [24]. An extrapolation to zero loading of the results will eliminate this effect. In conclusion, $j_{Pt}(5\%)$ matches with the desired ORR kinetic current density, thus ensuring the accuracy of the framework described in Section 3 on implementation in practical systems [16]. Figure 1 shows the determination of $E(j_{Pt}(5\%))$ from CV-TF-RRDE profiles. Figure 3(a) summarizes the $E(j_{Pt}(5\%))$ of different 'model' ORR ECs in an alkaline environment (0.1 M KOH). This is meant to mimic the operating conditions that the EC would find at the cathode of an anion-exchange membrane fuel cell or of a metal-air battery. These ECs, which are selected representatives among the extremely broad variety of materials reported in the literature [39,40], consist of: (i) a conventional Pt/C benchmark with 10 wt% of Pt supported on Vulcan XC-72R, (ii) a 'Pt-free' EC of the type reported elsewhere [8]; and (iii) an advanced ORR EC comprising active sites based on a Pt—Ni alloy [41]. The 'Pt-free' EC and the advanced ORR EC comprising active sites based on a Pt—Ni alloy were obtained in our laboratory following the synthesis reported elsewhere [8,41].

For the sake of comparison, Figure 3(b) displays for the same ECs also the potential at half-wave, $E_{1/2}$. $E_{1/2}$ is the typical figure of merit commonly adopted in the literature for the comparison of the performance of different ORR ECs [42,43]. The values of $E(j_{Pt}(5\%))$ and $E_{1/2}$ are reported in Table 1 and shown in Figure 3(a) and (b), respectively.

For the selected EC, the current density at which $E_{1/2}$ is determined depends on the specific value of $j_{EC,d}$ and on several factors including the transport phenomena and,

Figure 3

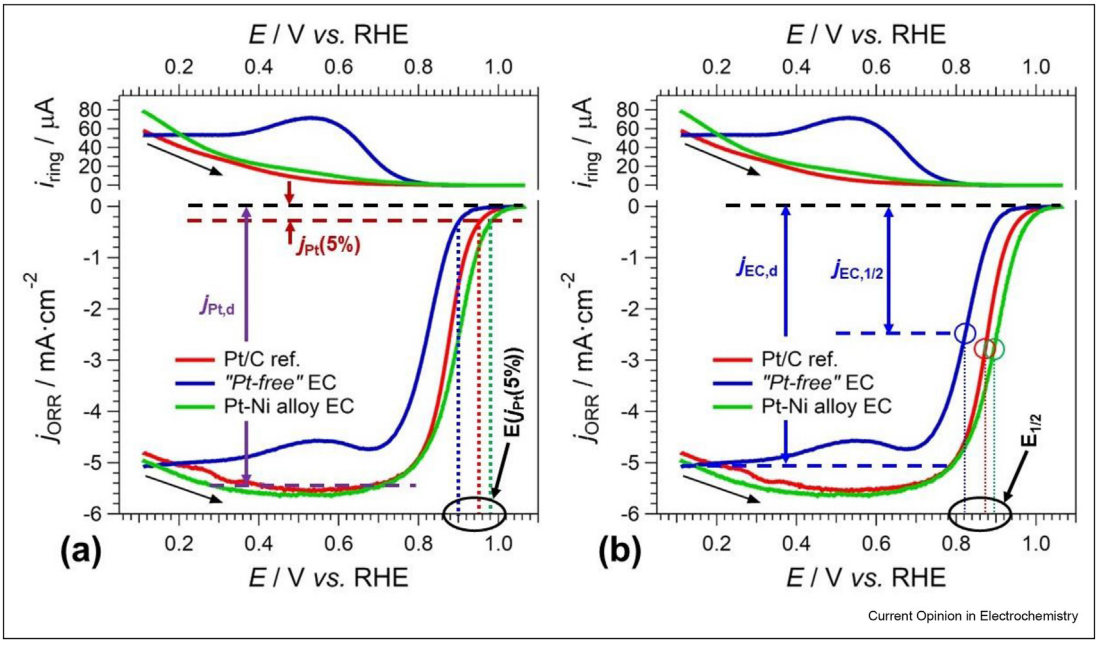

Comparison between $E(j_{Pt}(5\%))$ and $E_{1/2}$. (**a**) Determination of $E(j_{Pt}(5\%))$ values for selected ORR ECs. (**b**) Determination of $E_{1/2}$ values of selected ORR ECs. EC, electrocatalyst; ORR, oxygen reduction reaction.

Table 1

Comparison between E(j_{Pt}(5%)) and $E_{1/2}$ for a variety of 'model' ORR ECs.[a]

Electrocatalyst	E(j_{Pt}(5%))/mV *vs.* RHE	$E_{1/2}$/mV *vs.* RHE
Pt/C ref.	955	873
'Pt-*free*' EC	903	822
Pt–Ni alloy EC	983	895

EC, electrocatalyst; ORR, oxygen reduction reaction.
[a] Voltammograms measured at 20 mV/s; temperature = 298 K; support electrolyte = 0.1 M KOH; rotating speed 1600 rpm; E_{ring} = 1.2 V *vs.* RHE.

in accordance with the Levich analysis [27], the total number of electrons exchanged during the ORR. Figure 3 shows that, with respect to both the Pt/C benchmark and the Pt–Ni alloy EC, the 'Pt-free' EC produces a significant larger amount of H_2O_2 thus lowering the total number of exchanged electrons and consequently j_d. In addition, the current density ($j_{EC,1/2}$) at $E_{1/2}$ is *ca.* 10 times larger than that of j_{Pt}(5%). This has two important consequences.

i. The corrections that are necessary to determine the ORR kinetic current densities in an RRDE setup are significant: specifically, $j_{k,ORR} = 2 \cdot j_{EC,1/2}$, hence the correction to the measured current density is equal to 100%. In this range, even small errors in the determination of $j_{EC,d}$ affect significantly the accuracy of $j_{k,ORR}$ [16].
ii. $\frac{C_{ox,EC}(0,t)}{C_{ox,Pt}(0,t)} \neq 1$, since at large current densities the morphology of the ECs can easily lead to a different accessibility of O_2 to the active sites caused by mass transport issues. The contribution to the η_{EC} of resulting accessibility overpotential, η_A, is very significant (see Figure 2).

From these considerations, it is clear that $E_{1/2}$ is a very 'rough' and unsuitable figure of merit to adopt to compare the pure catalytic ORR activity of ECs. Indeed, in ECs, owing to their different compositions, structure and morphology with respect to reference material, the contribution of η_s and η_A to the $E_{1/2}$ is relevant. Taking all together, E(j_{Pt}(5%)) is an accurate figure of merit to gauge the 'pure' kinetic performance in the ORR of an EC as it is immediately correlated to the crucial catalytic feature of the material, that is, the activation free energy barrier of the EC.

Conclusions

This report describes a very general method to compare accurately the catalytic activity of different ECs. This method is based on a formalism which does not involve the usually-adopted Butler-Volmer description of electrocatalytic processes. This formalism takes into account that: (i) the rate constants of the elementary reduction and of the reverse oxidation processes at the interface during the EC operation can be different; and (ii) the concentration on the electrode of the oxidized and of the reduced species involved in the ORR are typically different. In principle, the method can be applied to most processes involved in the operation of electrochemical energy conversion and storage devices, on the condition that they trigger overpotentials larger than 100–150 mV. Hence, the formalism could be applied to diverse processes such as the ORR, the oxygen evolution reaction, and the methanol oxidation reaction, both in an aqueous and in a nonaqueous environment. It does not make any assumption on the specific features of the EC including the morphology and the chemical composition. The proposed formalism compares the potential of an EC with that of a benchmark EC both tested exactly in the same conditions and producing the same current density. Specifically, the method consists in the study of the CV-TF-RRDE profiles at a current density which is equal to 5% of the diffusion-limited ORR current density of a Pt benchmark (j_{Pt}(5%)). In this condition the measured electrode potential E(j_{Pt}(5%)) is correlated with the crucial features of an EC, such as: (i) the number of electrons exchanged in the ORR; (ii) the accessibility of O_2 to the active sites; and (iii) the kinetic activation barrier for the ORR. This correlation retains its accuracy regardless of the specific features of the EC, including the morphology and the chemical composition. It is also demonstrated that, with respect to other figures of merit discussed in the literature such as $E_{1/2}$, E(j_{Pt}(5%)) is a much more accurate and quantitative parameter to gauge the ORR kinetics of ECs. In summary the method here reported, by simple CV-TF-RRDE measurements, provides useful parameters able to shed light and identify which features characterizing an ORR EC need to be optimized for application into a practical electrochemical device.

Declaration of competing interest

The authors declare that they have no known competing financial interests or personal relationships that could have appeared to influence the work reported in this article.

Acknowledgements

This research has received funding from (a) the European Union's Horizon 2020 research and innovation program under grant agreement 881603 (b) the project 'Advanced Low-Platinum hierarchical Electrocatalysts for low-T fuel cells' funded by EIT Raw Materials, (c) Alkaline membranes and (platinum group metals)-free catalysts enabling innovative, open electrochemical devices for energy storage and conversion — AMPERE, FISR 2019 project funded by the Italian Ministry of University and Research, and (d) the project 'Hierarchical electrocatalysts with a low platinum loading

for low-temperature fuel cells — HELPER' funded by the University of Padova. PJK and IAR (University of Warsaw) were supported in part by the National Science Center (NCN, Poland) under Opus Project 2018/29/B/ST5/02627.

References

Papers of particular interest, published within the period of review, have been highlighted as:

* of special interest
** of outstanding interest

1. Buckingham R, Asset T, Atanassov P: **Aluminum-air batteries: a review of alloys, electrolytes and design**. *J Power Sources* 2021, **498**:229762.

2. Chin C-C, Yang H-k, Chen J: **Investigation of MnO_2 and ordered mesoporous carbon composites as electrocatalysts for Li-O_2 battery applications**. *Nanomaterials* 2016, **6**:21.

3]. * Lee J-S, Tai Kim S, Cao R, Choi N-S, Liu M, Lee KT, Cho J: **Metal–air batteries with high energy density: Li–air versus Zn–air**. *Adv Energy Mater* 2011, **1**:34–50.
This is a classic and comprehensive introduction on the fundamentals and applications of metal-air batteries.

4. Rahman MA, Wang X, Wen C: **A review of high energy density lithium–air battery technology**. *J Appl Electrochem* 2014, **44**:5–22.

5]. ** Wang Y-J, Fang B, Zhang D, Li A, Wilkinson DP, Ignaszak A, Zhang L, Zhang J: **A review of carbon-composited materials as air-electrode bifunctional electrocatalysts for metal–air batteries**. *Electrochem Energy Rev* 2018, **1**:1–34.
This review provides a modern and authoritative overview on the air electrodes of metal-air batteries, focusing on the different families of state-of-the-art electrocatalysts.

6. Di Noto V, Negro E, Nale A, Kulesza PJ, Rutkowska IA, Vezzù K, Pagot G: **Correlation between precursor properties and performance in the oxygen reduction reaction of Pt and Co "core-shell" carbon nitride-based electrocatalysts**. *Electrocatalysis* 2020, **11**:143–159.

7. Negro E, Bach Delpeuch A, Vezzù K, Nawn G, Bertasi F, Ansaldo A, Pellegrini V, Dembinska B, Zoladek S, Miecznikowski K, Rutkowska IA, Skunik-Nuckowska M, Kulesza PJ, Bonaccorso F, Di Noto V: **Toward Pt-free anion-exchange membrane fuel cells: Fe–Sn carbon nitride–graphene core–shell electrocatalysts for the oxygen reduction reaction**. *Chem Mater* 2018, **30**:2651–2659.

8. Vezzù K, Bach Delpeuch A, Negro E, Polizzi S, Nawn G, Bertasi F, Pagot G, Artyushkova K, Atanassov P, Di Noto V: **Fe-carbon nitride "Core-shell" electrocatalysts for the oxygen reduction reaction**. *Electrochim Acta* 2016, **222**:1778–1791.

9]. * Di Noto V, Negro E, Vezzu K, Bertasi F, Nawn G: **Origins, developments, and perspectives of carbon nitride-based electrocatalysts for application in low-temperature FCs**. *Interf Magaz* 2015, **24**:59–64.
This work introduces the fundamental background and the synthetic approaches involved in the preparation of electrocatalysts for the ORR comprising a carbon nitride matrix.

10. Negro E, VezzÙ K, Bertasi F, Schiavuta P, Toniolo L, Polizzi S, Di Noto V: **Interplay between nitrogen concentration, structure, morphology, and electrochemical performance of PdCoNi "core–shell" carbon nitride electrocatalysts for the oxygen reduction reaction**. *ChemElectroChem* 2014, **1**:1359–1369.

11. Sarapuu A, Kibena-Põldsepp E, Borghei M, Tammeveski K: **Electrocatalysis of oxygen reduction on heteroatom-doped nanocarbons and transition metal–nitrogen–carbon catalysts for alkaline membrane fuel cells**. *J Mater Chem* 2018, **6**:776–804.

12. Li R, Li C: **Chapter one - photocatalytic water splitting on semiconductor-based photocatalysts**. In *Advances in catalysis*. Edited by Song C, Academic Press; 2017:1–57.

13. Armstrong FA, Hirst J: **Reversibility and efficiency in electrocatalytic energy conversion and lessons from enzymes**. *Proc Natl Acad Sci Unit States Am* 2011, **108**:14049–14054.

14. Biemolt J, Douglin JC, Singh RK, Davydova ES, Yan N, Rothenberg G, Dekel DR: **An anion-exchange membrane fuel cell containing only abundant and affordable materials**. *Energy Technol* 2021, **9**:2000909.

15. Salonen LM, Petrovykh DY, Kolen'ko YV: **Sustainable catalysts for water electrolysis: selected strategies for reduction and replacement of platinum-group metals**. *Mater Today Sustain* 2021, **11–12**:100060.

16]. ** Di Noto V, Negro E, Nale A, Pagot G, Vezzù K, Atanassov P: **Hidden in plain sight: unlocking the full potential of cyclic voltammetry with the thin-film rotating (ring) disk electrode studies for the investigation of oxygen reduction reaction electrocatalysts**. *Curr Opin Electrochem* 2021, **25**:100626.
This work describes in detail: (i) the approaches needed to obtain an accurate evaluation of the faradic ORR currents in experiments carried out through cyclic voltammetry with the thin-film rotating ring-disk electrode (CV-TF-RRDE); and (ii) how to analyze CV-TF-RRDE data to expand the scope of this technique.

17. Kuzmin AV, Shainyan BA: **Theoretical density functional theory study of electrocatalytic activity of MN_4-doped (M = Cu, Ag, and Zn) single-walled carbon nanotubes in oxygen reduction reactions**. *ACS Omega* 2021, **6**:374–387.

18. Wang D, Pan X, Yang P, Li R, Xu H, Li Y, Meng F, Zhang J, An M: **Transition metal and nitrogen Co-doped carbon-based electrocatalysts for the oxygen reduction reaction: from active site insights to the rational design of precursors and structures**. *ChemSusChem* 2021, **14**:33–55.

19. Fernandez-Escamilla HN, Guerrero-Sanchez J, Contreras E, Ruiz-Marizcal JM, Alonso-Nunez G, Contreras OE, Felix-Navarro RM, Romo-Herrera JM, Takeuchi N: **Understanding the selectivity of the oxygen reduction reaction at the atomistic level on nitrogen-doped graphitic carbon materials**. *Adv Energy Mater* 2021, **11**:2002459.

20. Martin DJ, Wise CF, Pegis ML, Mayer JM: **Developing scaling relationships for molecular electrocatalysis through studies of Fe-Porphyrin-Catalyzed O_2 reduction**. *Accounts Chem Res* 2020, **53**:1056–1065.

21]. ** Liu T, Vivek JP, Zhao EW, Lei J, Garcia-Araez N, Grey CP: **Current challenges and routes forward for nonaqueous lithium–air batteries**. *Chem Rev* 2020, **120**:6558–6625.
This review article describes the fundamental concepts on the basis of the electrochemical reaction mechanisms characterizing the processes occurring in lithium-air batteries.

22. Wu G, Mack NH, Gao W, Ma S, Zhong R, Han J, Baldwin JK, Zelenay P: **Nitrogen-Doped graphene-rich catalysts derived from heteroatom polymers for oxygen reduction in nonaqueous lithium-O_2 battery cathodes**. *ACS Nano* 2012, **6**:9764–9776.

23. Xu Y, Shelton WA: **O_2 reduction by lithium on Au(111) and Pt(111)**. *J Chem Phys* 2010, **133**, 024703.

24. Sarapuu A, Hussain S, Kasikov A, Pollet BG, Tammeveski K: **Electroreduction of oxygen on Nafion®-coated thin platinum films in acid media**. *J Electroanal Chem* 2019, **848**:113292.

25. Curnick OJ, Pollet BG, Mendes PM: **Nafion®-stabilised Pt/C electrocatalysts with efficient catalyst layer ionomer distribution for proton exchange membrane fuel cells**. *RSC Adv* 2012, **2**:8368–8374.

26. Wang J, Zhao C-X, Liu J-N, Ren D, Li B-Q, Huang J-Q, Zhang Q: **Quantitative kinetic analysis on oxygen reduction reaction: a perspective**. *Nano Mater Sci* 2021 (in press).

27]. ** Bard AJ, Faulkner LR: *Electrochemical methods: fundamentals and applications*. 2nd ed. Wiley; 2000.
This is a cornerstone book in electrochemistry, which discusses the fundamental background and all the main methods that are commonly adopted to study the materials for electrochemical applications. This is an excellent reference both for the beginner who aims to understand fundamental electrochemistry and for the specialist who requires an advanced and detailed description of electrochemical phenomena.

28. Shinozaki K, Zack JW, Richards RM, Pivovar BS, Kocha SS: **Oxygen reduction reaction measurements on platinum electrocatalysts utilizing rotating disk electrode technique**. *J Electrochem Soc* 2015, **162**:F1144–F1158.

29. Zana A, Wiberg GKH, Arenz M: **Oxygen reduction reaction on polycrystalline platinum: on the activity enhancing effect of polyvinylidene difluoride**. *Surfaces* 2019, **2**:69–77.

30. Halseid R, Bystroň T, Tunold R: **Oxygen reduction on platinum in aqueous sulphuric acid in the presence of ammonium**. *Electrochim Acta* 2006, **51**:2737–2742.

31. Tan A-d, Wang Y-f, Fu Z-y, Tsiakaras P, Liang Z-x: **Highly effective oxygen reduction reaction electrocatalysis: nitrogen-doped hierarchically mesoporous carbon derived from interpenetrated nonporous metal-organic frameworks**. *Appl Catal B Environ* 2017, **218**:260–266.

32]. * Trasatti S: **Reaction mechanism and rate determining steps**. In *Handbook of fuel cells - fundamentals technology and applications*. Edited by Vielstich W, Lamm A, Gasteiger HA, Chichester: John Wiley & Sons; 2003:79–87.
This chapter offers a detailed theoretical discussion on the fundamental mechanisms and reaction kinetics of the electrochemical processes.

33]. ** Sepa DB, Vojnovic MV, Vracar LM, Damjanovic A: **Different views regarding the kinetics and mechanisms of oxygen reduction at Pt and Pd electrodes**. *Electrochim Acta* 1987, **32**: 129–134.
This fundamental work provides a detailed description of the ORR mechanism as a function of pH and electrochemical potential.

34]. * O'Hayre R, Cha S-W, Colella W, Prinz FB: *Fuel cell fundamentals*. 3rd ed. ed. Hoboken: John Wiley & Sons; 2016.
This is a classic and comprehensive introduction on the fundamentals and applications of fuel cells.

35. Lim D-H, Wilcox J: **Mechanisms of the oxygen reduction reaction on defective graphene-supported Pt nanoparticles from first-principles**. *J Phys Chem C* 2012, **116**:3653–3660.

36]. ** Schmidt TJ, Gasteiger HA: **Rotating thin-film method for supported catalysts**. In *Handbook of fuel cells - fundamentals, technology and applications*. Edited by Vielstich V, Lamm A, Gasteiger HA, Chichester: John Wiley & Sons; 2003:316–333.
This chapter provides an extensive description of the fundamentals and applications of cyclic voltammetry with the thin-film rotating ring-disk electrode technique to study electrochemical processes and electrocatalysts.

37. Kuang M, Wang Q, Han P, Zheng G: **Cu, Co-embedded N-enriched mesoporous carbon for efficient oxygen reduction and hydrogen evolution reactions**. *Adv Energy Mater* 2017, **7**:1700193.

38. Li Z, Zeng R, Wang L, Jiang L, Wang S, Liu X: **A simple strategy to form hollow Pt3Co alloy nanosphere with ultrathin Pt shell with significant enhanced oxygen reduction reaction activity**. *Int J Hydrogen Energy* 2016, **41**:21394–21403.

39]. * Martinez U, Komini Babu S, Holby EF, Chung HT, Yin X, Zelenay P: **Progress in the development of Fe-based PGM-free electrocatalysts for the oxygen reduction reaction**. *Adv Mater* 2019, **31**:1806545.
Fe-Based "PGM-free" electrocatalysts for the ORR are compared and their properties and performance are highlighted. These materials show an interesting and promising electroactivity in the investigated application.

40]. * Kim C, Dionigi F, Beermann V, Wang X, Möller T, Strasser P: **Alloy nanocatalysts for the electrochemical oxygen reduction (ORR) and the direct electrochemical carbon dioxide reduction reaction (CO_2RR)**. *Adv Mater* 2019, **31**:1805617.
This work provides excellent insight into alloy nanocatalysts, that are highly relevant for different electroreduction reactions.

41. Di Noto V, Negro E, Gliubizzi R, Gross S, Maccato C, Pace G: **Pt and Ni carbon nitride electrocatalysts for the oxygen reduction reaction**. *J Electrochem Soc* 2007, **154**:B745–B756.

42. Brocato S, Serov A, Atanassov P: **PH dependence of catalytic activity for ORR of the non-PGM catalyst derived from heat-treated Fe-phenanthroline**. *Electrochim Acta* 2013, **87**: 361–365.

43. Zhang J, Lv M, Liu D, Du L, Liang Z: **Nitrogen-doped carbon nanoflower with superior ORR performance in both alkaline and acidic electrolyte and enhanced durability**. *Int J Hydrogen Energy* 2018, **43**:4311–4320.